Published in final edited form as:
Oncogene. 2015 November 19; 34(47): 5821–5831. doi:10.1038/onc.2015.34.

Blocking CLEC14A-MMRN2 binding inhibits sprouting angiogenesis and tumour growth

Noy PJ[1], **Lodhia P**[1], **Khan K**[1], **Zhuang X**[1], **Ward DG**[2], **Verissimo AR**[1], **Bacon A**[3], and **Bicknell R**[1]

[1]Angiogenesis Laboratory, Institute for Biomedical Research, Schools of Immunity and Infection and Cancer Sciences, College of Medical and Dental Sciences, University of Birmingham, UK

[2]Institute of Cancer Studies, School of Cancer Sciencies, University of Birmingham, UK

[3]School of Immunity and Infection, Institute for Biomedical Research, The Medical School, University of Birmingham, UK

Abstract

We previously identified CLEC14A as a tumour endothelial marker. Here we show CLEC14A is a regulator of sprouting angiogenesis *in vitro* and *in vivo*. Using a HUVEC spheroid sprouting assay we found CLEC14A to be a regulator of sprout initiation. Analysis of endothelial sprouting in aortic ring and *in vivo* subcutaneous sponge assays from *clec14a*$^{+/+}$ and *clec14a*$^{-/-}$ mice revealed defects in sprouting angiogenesis in CLEC14A deficient animals. Tumour growth was retarded and vascularity reduced in *clec14a*$^{-/-}$ mice. Pulldown and co-immunoprecipitation experiments confirmed MMRN2 binds to the extracellular region of CLEC14A. The CLEC14A-MMRN2 interaction was interrogated using mouse monoclonal antibodies. Monoclonal antibodies were screened for their ability to block this interaction. Clone C4 but not C2 blocked CLEC14A-MMRN2 binding. C4 antibody perturbed tube formation and endothelial sprouting *in vitro* and *in vivo*, with a similar phenotype to loss of CLEC14A. Significantly, tumour growth was impaired in C4 treated animals and vascular density was also reduced in the C4 treated group. We conclude that CLEC14A-MMRN2 binding has a role in inducing sprouting angiogenesis during tumour growth, that has the potential to be manipulated in future anti-angiogenic therapy design.

Keywords

Anti-angiogenic therapy; CLEC14A KO mouse; therapeutic antibodies

Corresponding Author: Roy Bicknell, Angiogenesis Laboratory, Institute for Biomedical Research, The Medical School, University of Birmingham, Edgbaston, Birmingham B15 2TT, UK, Telephone: (44)-121-4144085, r.bicknell@bham.ac.uk.

Conflict of interest: RB and XZ are named inventors of a patent filed by Cancer Research UK in the United States Patent and trademark Office on 3 September 2009 under No. 61/239,584, bearing Attorney Docket No. P0357.70004US00 and entitled ‘Inhibitors’. All the other authors declare no conflict of interest.

Europe PMC Funders Author Manuscripts

Introduction

It is well established that solid tumour growth relies on the recruitment of endothelial cells and ultimately blood vessels from the surrounding healthy tissue. These recruited blood vessels deliver oxygen and nutrients, through blood flow, to the tumour. A primary mechanism of this recruitment is through sprouting angiogenesis of vessels adjacent to the tumour arising from tumour-derived release of VEGF. Sprouting angiogenesis is a tightly regulated process, where the main regulatory components are VEGFR2, Notch and Angpoietin/Tie2 signalling pathways with cross-talk been these systems essential for direction, growth and cell specification.[1,2] However, recent studies have highlighted the role of multiple other pathways as regulators of this process, including factors involved in glycolysis,[3] PKA signalling,[4] as well as new regulators of extracellular matrix composition.[5,6] Manipulation of these factors has also been shown to suppress angiogenic sprouting *in vitro* and *in vivo*.

Targeting angiogenesis in cancer has many therapeutic advantages, including efficient delivery to target tissue type, stable genetic profile, and lower potential for side effects than conventional chemotherapy. Current anti-angiogenic therapies in the clinic primarily target the VEGF signalling pathway, but with limited success.[7] More recent efforts to develop effective anti-angiogenic therapies have focussed on understanding and targeting the endothelial tip and stalk cells during sprouting angiogenesis.[2] For this to be effective, greater knowledge is required to understand the pathways involved in tip cell formation and behaviour.

CLEC14A is a single-pass transmembrane glycoprotein that belongs to the vascular expressed C-type lectin family 14, whose other members include CD248/TEM1/Endosialin, Thrombomodulin and CD93.[8] Although functionally CLEC14A is relatively unstudied, available data suggests that manipulation of CLEC14A levels or function blocking antibodies will regulate endothelial migration possibly through an interaction with the extracellular matrix.[9-12] CLEC14A was originally identified to be an endothelial specific gene that is highly upregulated on vessels associated with multiple solid tumours.[9] More recent work has shown CLEC14A as part of a “common angiogenesis signature” in a meta-analysis of 121 head and neck squamous cell carcinomas, 959 breast cancers and 170 clear cell renal cell carcinomas.[13] MMRN2, an endothelial specific member of the emilin family and component of the extracellular matrix,[14,15] was recently found as an extracellular interacting protein for CLEC14A and MMRN2 and CLEC14A were both upregulated in tumour vasculature during tumour progression.[11] Thus, although it is becoming apparent that CLEC14A has a likely function in the tumour vasculature our knowledge is restricted. In this study we have investigated CLEC14A in sprouting angiogenesis and for the first time examined its role *in vivo*.

Results

CLEC14A regulates sprouting angiogenesis *in vitro*

We previously described a role for CLEC14A in endothelial migration and tube formation *in vitro*.[9] To investigate the role of CLEC14A in sprouting angiogenesis *in vitro*, HUVEC

spheroids were generated from HUVECs treated with siRNAs targeting *clec14a* or a non-complementary siRNA duplex. Knockdown of *clec14a* expression was confirmed at the mRNA level by qPCR for both *clec14a* targeted siRNAs with an average reduction of 84% and 83% across three experiments (Figure 1A) and at the protein level by Western blot analysis of protein extracts probed with an anti-CLEC14A polyclonal antisera (Figure 1B). VEGF induced sprouting from CLEC14A knockdown spheroids was impaired, knockdown spheroids produced on average 6.9 or 6.4 sprouts per spheroid for duplex 1 or 2 respectively, compared to 13.2 for control cells (Figures 1C and 1D). To determine the role of CLEC14A in tip/stalk cell formation, control HUVECs and knockdown HUVECs were stained either red or green and mixed, prior to spheroid formation and induced sprouting (Figure 1E). Knockdown of CLEC14A reduced the percentage of cells at the tip position (33%) compared to control cells (67%), however, there was no effect on the percentage of stalk cells that were derived from CLEC14A knockdown HUVECs (Figure 1F). These data suggest CLEC14A has a role in sprout initiation and migration.

CLEC14A regulates sprouting angiogenesis *in vivo*

Previously published data for CLEC14A has demonstrated its role in endothelial biology *in vitro*, however its *in vivo* role has not been reported. To investigate the role of CLEC14A *in vivo* and *ex vivo*, mice were generated to replace the *clec14a* coding sequence with a *lacZ* reporter (Figure 2A). Breeding was normal (Supplemental Table 1). Aortas were isolated from *clec14a*$^{+/+}$ and *clec14a*$^{-/-}$ mice. Extracted cDNA was analysed by qPCR and confirmed loss of the *clec14a* coding region but expression of the 5′ and 3′ untranslated regions were retained (Figure 2B) and expression of *mmrn2* was unaltered (Supplemental Figure 1). Loss of CLEC14A at the protein level was also confirmed by Western blot analysis of lung tissue lysates (Figure 2C).

To confirm the role of CLEC14A in sprouting angiogenesis in a multicellular three dimensional co-culture, aortas were isolated, cut into rings and embedded in collagen. Cellular outgrowth was stimulated by VEGF and monitored over 7 days before end-point quantitation of endothelial sprouting. Again, loss of CLEC14A impaired endothelial sprout outgrowth and migration (Figure 2D). Aortic rings from wildtype mice produced over double the number of tubes compared to that observed for CLEC14A knockout mice (30.6 tubes compared to 13.4 tubes respectively) (Figure 2E). In addition, the maximum migration, which is defined by the furthest distance migrated away from each aortic ring, was also reduced in knockout cultures (Figure 2F). To assess whether CLEC14A has a similar function *in vivo*, sponge barrels were implanted subcutaneously into CLEC14A knockout mice. Cellular infiltration and neo-angiogenesis were stimulated using bFGF injections into the sponge every two days for two weeks. Macroscopic analysis of sponge sections stained with haematoxylin and eosin revealed impaired infiltration of cells into the sponge in *clec14a*$^{-/-}$ animals (Figures 2G and 2H). In addition, vascularity was significantly reduced ($p<0.01$) for *clec14a*$^{-/-}$ animals (Figure 2I). To confirm the endothelial cells lining the neoangiogenic vessels express *clec14a* in this model, sponges and livers from CLEC14A KO mice were stained with x-gal. Strong x-gal staining was observed on blood vessels within the sponge compared to matched liver sections (Figure 2J). From these data we can conclude that mouse CLEC14A expression regulates endothelial migration and angiogenic

Europe PMC Funders Author Manuscripts

sprouting *in vivo*, as well as *in vitro*, and CLEC14A is upregulated on sprouting endothelium.

CLEC14A promotes tumour growth

CLEC14A expression is found highly up-regulated on human tumour vessels compared to vessels from healthy tissue, suggesting that cancer therapies could be targeted against CLEC14A.[9] Therefore, to investigate whether loss of CLEC14A effects tumour growth, we used the syngeneic Lewis lung carcinoma (LLC) model. For this 1×10^6 LLC cells were injected subcutaneously into the right flank of either *clec14a*$^{+/+}$ or *clec14a*$^{-/-}$ mice. Tumour growth was impaired in the *clec14a*$^{-/-}$ mice compared to *clec14a*$^{+/+}$ littermates (Figure 3A). This was confirmed by three independent experiments. Excised tumours taken from *clec14a*$^{-/-}$ mice were smaller in size (Figure 3B) and smaller in weight (Figure 3C) than *clec14a*$^{+/+}$ littermates. To determine whether the vascular density within these tumours was also effected, tissue sections were stained with an anti-CD31 antibody. Analysis shows a reduced density of discrete vessels (Figures 3D and 3E) and reduced percentage endothelial coverage (Figure 3F). In healthy tissues, highest expression of x-gal in sections from *clec14a*$^{-/-}$ mice was seen in the liver vessels (black arrow) but was vastly less than that seen on both mature vessels, with erythrocyte filled lumens (Figure 3G, black arrows), and immature microvessels within the tumour (Figure 3G, red arrows), confirming *clec14a* is upregulated on tumour vessels.

Identification and confirmation of CLEC14A-MMRN2 interaction

To identify potential binding partners for the extracellular domain for CLEC14A, we first purified CLEC14A extracellular domain protein tagged with human Fc. This protein or Fc alone was incubated with HUVEC whole cell lysates and precipitated using protein A agarose beads. The precipitated proteins were then washed and separated on a SDS-PAG. Seven gel regions were excised, digested and analysed by mass spectrometry. The most abundant protein identified was MMRN2 with 12 peptides (11 unique), and no peptides in the corresponding control pulldown fraction. Western blot analysis of the precipitates confirmed the presence of MMRN2 in the CLEC14A-ECD-Fc pull-down and was not detected in the Fc alone pull-down (Figure 4A). To further confirm this interaction, endogenous CLEC14A was immunoprecipitated from HUVEC whole cell lysates. Western blot analysis confirmed MMRN2 co-precipitation in the CLEC14A precipitate but was not detected in the IgG control (Figure 4B).

Development and validation of CLEC14A monoclonal antibodies

To further our understanding of CLEC14A, we next produced cross-species reactive antibodies. To enable this, murine CLEC14A protein with a human Fc tag was expressed in HEK293T cells and purified on a protein A column. Mice were then immunised with 50 μg mCLEC14A with complete Freund's adjuvant to break tolerance. Clones were screened for activity against human CLEC14A or human Fc. To confirm the clones could recognise cell bound CLEC14A, HEK293T cells overexpressing HA-CLEC14A were stained with clone C2 or C4 or a monoclonal HA tag antibody. FACs analysis shows increased fluorescence for each of the antibodies in the HA-CLEC14A overexpressing cells compared to control transfected cells (Figure 5A). To confirm that antibodies recognise the endogenous form of

Europe PMC Funders Author Manuscripts

CLEC14A, these clones were used to stain HUVEC treated with control or *clec14a* targeted siRNAs. Control HUVEC were stained strongly by clone C2 and C4 and this staining was reduced to isotype control levels by knockdown of CLEC14A (Figure 5B). These results confirmed the specificity of the CLEC14A monoclonal antibodies.

To determine whether the C2 and C4 clones bind to the same region of CLEC14A, HUVECs were pre-treated with BSA, C2 or C4 antibody prior to C2-FITC staining. C2 incubation blocked C2-FITC staining effectively, but C4 had little effect (Figure 5C). The same pre-treatment was repeated prior to C4-FITC staining. C2 antibody did not effect C4-FITC staining however, HUVECs pre-treated with C4 showed reduced binding of C4-FITC (Figure 5D). From these results we can conclude that C2 and C4 bind to discrete regions of CLEC14A.

A CLEC14A monoclonal antibody blocks CLEC14A-MMRN2 binding

To determine whether either of these CLEC14A monoclonal antibodies could inhibit the binding of MMRN2 to CLEC14A, CLEC14A-ECD-Fc was pre-incubated with increasing concentrations of mIgG1, or C2, or C4, prior to incubation with lysates from HEK293T cells overexpressing MMRN2. Precipitates were then separated and probed for MMRN2 or CLEC14A-ECD-Fc. MMRN2 binding was observed for CLEC14A-ECD-Fc precipitates blocked with mIgG1 or C2 (Figure 5E) but no MMRN2 binding was observed in the C4 blocked precipitates (Figure 5F). This confirms that the C4 but not the C2 monoclonal antibody blocks MMRN2 binding to CLEC14A.

CLEC14A-MMRN2 blocking antibody inhibits tube formation and sprouting angiogenesis *in vitro* and *in vivo*

We previously showed that CLEC14A expression regulates endothelial cell migration and tube formation.[9] To assess whether C2 or C4 have a role in modulating endothelial cell migration, wounds were scratched into HUVEC monolayers and treated with 20 μg/ml mIgG1, C2 or C4. Wound closure was assessed at 16-24 hours. However, no difference was observed between any of the treatments (data not shown). Antibody treatment also had no effect on CLEC14A expression (Supplemental Figure 2). To determine whether the CLEC14A monoclonal antibodies have regulatory properties in *in vitro* tube formation, HUVECs were plated onto Matrigel and treated with either mIgG1, C2 or C4 for 16hrs. The C2 treatment had no effect on tube formation compared to the mIgG1 control; however, C4 treatment effected branching and meshes (Figure 6A). The number of meshes (Figure 6B) was decreased in the C4 treatment group, with a corresponding increase in the number of branches (Figure 6C) for this treatment group compared to the control and C2 groups. Furthermore, C4 treated HUVECs have decreased branch length (Figure 6D). These data suggest that C4 inhibits the sprouting or sensing and delays interconnectivity of the tubes, but the second CLEC14A targeted antibody (C2) was without activity on tube formation.

To investigate how disruption of the MMRN2-CLEC14A interaction effects sprouting *in vitro*, we treated HUVEC spheroids with 20 μg/ml C4 or C2 or mIgG1 control antibodies. Control, mIgG1 treated, spheroids formed sprouts after 16 hours as expected (Figure 6E). C2 treatment had no effect on sprouting, but C4 treatment inhibited sprout formation by

Europe PMC Funders Author Manuscripts

50 % (Figures 6E and 6F). To further investigate, aortic ring cultures were also supplemented with 20 μg/ml C4 or C2 or mIgG1 antibodies. Endothelial outgrowth and tube formation was well established after 7 days culture in the presence of mIgG1 (Figure 6G). C4 antibody effectively inhibited tube outgrowth, however C2 antibody was inactive in regulating tube/sprout formation from aortic rings (Figures 6G and 6H).

To confirm the importance of MMRN2, HUVECs were treated with *mmrn2* targeted siRNA or a control siRNA duplex. Knockdown of *mmrn2* expression was confirmed by qPCR (Figure 6I). Endothelial sprouting from MMRN2 knockdown HUVEC spheroids formed 8.9 (duplex 1) or 8.6 (duplex 2) sprouts per spheroid, compared to 15.7 for control spheroids (Figure 6J).

To evaluate the role of the MMRN2-CLEC14A interaction *in vivo*, subcutaneous sponge implants were used. Sponge infiltration was stimulated as previously described with the addition of either 10 μg mIgG1 or C4 antibody. Total cellular sponge infiltration was significantly reduced ($p<0.01$) in the C4 treatment group compared to the mIgG1 controls (Figures 6K and 6L). Vascular density of the invaded sponge was also reduced for the C4 antibody group (Figure 6M). These data demonstrate that the MMRN2-CLEC14A interaction promotes *in vivo* angiogenesis.

CLEC14A-MMRN2 blocking antibody inhibits tumour growth

As CLEC14A expression is most abundant on tumour endothelial cells and CLEC14A expression is associated with MMRN2 in tumours,[11] we hypothesised that disruption of this interaction would perturb tumour growth. Therefore, mice with LLC tumours were injected intraperitoneally twice per week with 10 μg C4 or mIgG1 (control) for the duration of the experiment. Tumour growth was slowed for mice treated with C4 antibody compared to the control, mIgG1, treatment group (Figure 7A). Tumours from the C4 treated mice were smaller in size (Figure 7B) and weight (Figure 7C) than control animals. Again we examined the vascular density within these tumours. Tissue sections were stained with an anti-CD31 antibody and fluorescent analysis revealed a reduced density of discrete vessels (Figures 7D and 7E) and the percentage endothelial coverage (Figure 7F). Suggesting that CLEC14A binding to MMRN2 is an important functional component of tumour induced angiogenesis.

Discussion

CLEC14A is one of a small group of endothelial genes that contribute to tumour angiogenesis in multiple tumour types.[9,13] Here we demonstrate that through loss of CLEC14A, tumour growth is inhibited *in vivo* (Figure 3). A similar phenotype has also been observed for other tumour endothelial markers, such as TEM8,[16] Endoglin,[17] Galectin,[18] ELTD1,[13] and Endosialin,[19] this demonstrates the importance of these tumour endothelial expressed genes in vascularisation and tumour growth. Although many groups have focused on factors involved in physiological sprouting angiogenesis, these tumour endothelial expressed genes could deliver tumour anti-angiogenic therapeutic potential.[20]

Upregulation of CLEC14A has been observed in human tumours[9,13,21] and murine models of pancreatic and cervical cancer[11] which supports our findings that *clec14a* expression is upregulated on tumour vessels in the LLC model (Figure 3). CLEC14A has been shown to regulate multiple aspects of endothelial biology including adhesion,[10,12] migration,[9,10,12] tube formation,[9-11] and we now demonstrate, as we first predicted,[22] it is also important for sprouting angiogenesis *in vitro* and *in vivo* (Figures 1 and 2). We can infer that this role of CLEC14A is through endothelial-endothelial interactions or endothelial-extracellular matrix interactions, because *in vitro* HUVEC sprouting is perturbed by CLEC14A knockdown, suggesting the presence of other cell types is dispensable. We also observed for the first time upregulation of *clec14a* expression on neoangiogenic vessels in the subcutaneous sponge assay (Figure 2). This is expected as newly formed endothelial sprouts have been modelled to experience extremely low shear stress (0.2 Pa) from the 4.2 μm of the bifurcation point to the tip of the sprout,[23] and *clec14a* expression is known to be upregulated by low shear stress.[9] Therefore, it is possible that CLEC14A has a role in regulating physiological sprouting angiogenesis also, however, its role will likely be limited by the co-expression of MMRN2.

Zanivan et al. identified MMRN2 as a component of the extracellular matrix that interacts with CLEC14A.[11] We independently verified this interaction through pulldown of proteins from HUVEC lysates using the extracellular domain of CLEC14A, as well as co-immunoprecipitation of the endogenous proteins (Figure 4). Through the generation and validation of CLEC14A monoclonal antibodies, we identified two antibodies that bind to discrete regions of CLEC14A (Figure 5C and 5D) and have shown that the C4 but not the C2 clone blocks the interaction of CLEC14A with MMRN2 (Figure 5E and 5F). To probe the function of the CLEC14A-MMRN2 interaction, we used the C4 antibody in Matrigel tube forming assays and found an increase in branching and decrease in evolved meshes (Figure 6). Knockdown by siRNA or targeting with polyclonal CLEC14A antisera has a similar effect on branching in this *in vitro* Matrigel assay.[9] However, another monoclonal antibody that binds CLEC14A but does not block MMRN2 binding had no effect (Figure 6). In a study using phage display to develop IgGs targeting the c-type lectin domain (CTLD) of CLEC14A, some of the generated IgGs reduced HUVEC cell migration and tube formation, although not all of the clones tested.[12] As our monoclonal antibody has a similar function it is possible that the MMRN2 binding site is within the CTLD region of CLEC14A, although further work is required to confirm this. *In vitro* and *in vivo* sprouting assays treated with C4 antibodies also demonstrated the role of the CLEC14A-MMRN2 interaction for endothelial sprouting (Figure 6). Lorenzon et al previously observed anti-angiogenic activity with soluble MMRN2 protein.[33] This data supports our model, as soluble MMRN2 protein could be binding to CLEC14A and disrupting the interaction of CLEC14A with MMRN2 in the extracellular matrix (Figure 8). Finally, we found that the CLEC14A-MMRN2 interaction is important for tumour growth (Figure 7), C4 treatment recapitulated tumour growth and reduced tumour vascularity as seen in *clec14a*$^{-/-}$ mice (Figure 3). Antibody inhibition of tumour endothelial marker function has been suggested as a mode of anti-angiogenic therapy for TEM8[24] and our studies corroborate this approach. Although in this example no ligand or mode of activity was identified. This is the first time that CLEC14A and a specific

extracellular interaction has been shown to be important for tumour growth, and suggests a hitherto unknown avenue into new anti-angiogenic therapies.

Materials and Methods

Reagents

For Western blotting and immunoprecipitation; primary antibodies: sheep polyclonal anti-human CLEC14A (R&D systems), mouse monoclonal anti-human Tubulin (Sigma), mouse polyclonal anti-human MMRN2 (Abnova); secondary antibodies: goat polyclonal anti-mouse IgG conjugated to horseradish peroxidase (HRP) (Dako), donkey polyclonal anti-sheep IgG conjugated to HRP (R&D systems). For immunofluorescence; primary antibodies: rabbit polyclonal anti-murine PECAM (Santa Cruz); secondary antibodies: donkey polyclonal anti-rabbit conjugated to Alexa Fluor488 (Invitrogen). For flow cytometry; primary antibodies: mouse monoclonal anti-HA tag (CRUK), mouse monoclonal anti-CLEC14A (C2, C4 described below); secondary antibodies: goat polyclonal anti-mouse IgG conjugated to Alexa Fluor488 (Invitrogen).

Plasmids

For protein production; lentiviral plasmids psPAX2 (lentiviral packaging; Addgene), pMD2G (Envelope plasmid; Addgene) and pWPI hCLEC14A-ECD-Fc (lentiviral mammalian expression plasmid containing IRES-EGFP; Addgene) were used. pWPI hCLEC14A-Fc and mCLEC14A-Fc was generated by initial PCR subcloning from *clec14a* IMAGE clone (Origene) into pcDNA3-Fc plasmid. The primers used were as follows: human CLEC14A fwd - 5′TAGTAGGAATTCGAGAGAATGAGGCCGGCGTTCGCCCTG3′; human CLEC14A rev - 5′AGAACCGCGGCCGCTGGAGGAGTCGAAAGCCTGAGGAGT3′; murine CLEC14A fwd - 5′TAGTAGGAATTCGAGAGAATGAGGCCAGCGCTTGCCCTG3′; murine CLEC14A rev - 5′CTACTAGCGGCCGCTCGTGGAAGAGGTGTCGAAAGT3′. EcoR1 and Not1 restriction sites were used to insert CLEC14A. A further round of PCR subcloning was performed to transfer the CLEC14A-Fc fusion into pWPI. The primers used were as follows: human CLEC14A fwd - 5′TAGTAGTTAATTAAGAGAGAATGAGGCCGGCGTTC3′; murine CLEC14A fwd - 5′TAGTAGTTAATTAAGAGAGAATGAGGCCAGCGCTT3′; human Fc rev - 5′CTACTAGTTTAAACTCATTTACCCGGAGACAGGGA3′. For this step, Pac1 and Pme1 restriction sites were used.

MMRN2 mammalian expression plasmid was constructed by PCR cloning from *mmrn2* IMAGE clone (Thermo) into pHL-Avitag3,[25] using the following primers: fwd - CCGGACCGGTCAGGCTTCCAGTACTAGCC; rev - CGGGGTACCGGTCTTAAACATCAGGAAGC. Age1 and Kpn1 restriction enzymes were used.

Europe PMC Funders Author Manuscripts

Cell culture

Human Umbilical Vein Endothelial Cells were isolated as described previously.[9] Umbilical cords were obtained from Birmingham Women's Health Care NHS Trust with informed consent. HUVECs and HEK293T cells were cultured as previously described.[34]

SiRNA transfections in HUVEC were performed as previously described for *clec14a*.[9] For *mmrn2* pre-designed siRNA duplexes were used (Ambion silencer select - ID S36387 and S36388). Lentivirus was produced in HEK293T cells by transient transfection with the lentiviral packaging, envelope and expression plasmids above. Plasmids were incubated in OptiMEM (Invitrogen) with polyethylenimine (36 μg/ml) at a 1:4 ratio for 10 minutes at room temperature prior to adding to HEK293T cells in cDMEM. Media supernatant was used to transduce fresh HEK293T cells. GFP positive HEK293T cells were sorted and used for protein production. Expression of MMRN2 in HEK293T cells was achieved by polyethylenimine transient transfection as above using pHL-Avitag3 hMMRN2.

Quantitative PCR

cDNA was prepared using the High-Capacity cDNA Archive kit (Applied Biosystems), from 1 μg of extracted total RNA. qPCR reactions were performed with Express qPCR supermix (Invitrogen) on a RG-3000 (Corbett, Manchester, UK) thermocycler. Primers for human *clec14a* and *flotillin-2* were as previously described.[9] Primers for murine *clec14a* 5′ UTR, CDS and 3′ UTR and murine beta-actin, are as follows: 5′UTR fwd - TTCCTTTTCCAGGGTTTGTG; 5′ UTR rev - GCCTACAAGGTGGCTTGAAT; CDS fwd - AAGCTGTGCTCCTGCTCTTG; CDS rev - TCCTGAGTGCACTGTGAGATG; 3′ UTR fwd - CTGTAGAGGGCGGTGACTTT; 3′ UTR rev - AGCTGCTCCCAAGTCCTCT; mACTB fwd - CTAAGGCCAACCGTGAAAAG; mACTB rev - ACCAGAGGCATACAGGGACA. Relative expression ratios were calculated according to the efficiency adjusted mathematical model.[27]

Western blotting and immunoprecipitation

Whole cell protein lysates were made and co-immunoprecipitation experiments were performed as previously described,[28] except protein was extracted from 2×10^7 HUVECs. For initial isolation of CLEC14A interacting proteins 5 μg CLEC14A-Fc or an equimolar amount of hFc was used. For endogenous immunoprecipitation experiments 0.4 μg anti-CLEC14A antibody or sheep IgG was used. For blocking experiments 5 μg CLEC14A-Fc or hFc were bound to protein G beads overnight in PBS. Beads were blocked for 5-6 hours in PBS containing 20 % FCS (PAA). Bound CLEC14A-Fc or hFc protein was blocked with increasing concentrations of mIgG, C2 or C4 in binding buffer overnight. Lysates from MMRN2 transfected HEK293T cells were then incubated overnight with the bead complexes before washing and analysing by Western blot. Standard protocols were used for Western blotting and SDS-PAGE.

Flow cytometry

Cells were detached with cell dissociation buffer (Invitrogen), rinsed in PBS before incubation in blocking buffer (PBS, 3 % BSA, 1 % NaN_3) for 15 minutes. Subsequent staining using 10 μg/ml anti-HA tag (CRUK), 10 μg/ml anti-CLEC14A (C2, C4 described

below), as primary antibodies, in blocking buffer for 30 minutes. Cells were rinsed in PBS and stained with goat polyclonal anti-mouse IgG conjugated to Alexa Fluor488 (Invitrogen) in blocking buffer. Data (15,000 events/sample) were collected using a FACSCalibur apparatus (Becton Dickinson, Oxford, UK), and results were analysed with Becton Dickinson Cell Quest software.

HUVEC spheroid sprouting assay and *in vitro* Matrigel tube forming assay

Generation of HUVEC spheroids and induction of endothelial sprouting in a collagen gel was performed as previously described,[29] using 1000 HUVECs per spheroid. Quantification was performed 16 hours after embedding. To quantify sprout growth the number of sprouts were counted, the cumulative sprout length and the maximal sprout length was assessed. For two colour sprouting experiments, HUVECs were pre-labelled with orange and green CellTracker dyes (Invitrogen). After 24 hours spheroids were fixed in 4% formaldehyde and mounted with Vectorshield (Vector labs). Slides were imaged with an Axioskop2 microscope and AxioVision SE64 Rel4.8 software (Zeiss, Cambridge, UK).

For the Matrigel tube forming assays 1.4×10^5 HUVECs were seeded onto 70 μl basement membrane extract (Matrigel, BD Bioscience) in a 12 well plate. After 16 hours, images were taken of 5 fields of view per well using a Leica DM IL microscope (Leica, Milton Keynes, UK) with a USB 2.0 2M Xli digital camera (XL Imaging LLC, Carrollton, TX, USA) at 10× magnification. Images were analysed with the Angiogenesis analyser plugin for Image J (Carpentier G. et al., Angiogenesis Analyzer for ImageJ. 4th ImageJ User and Developer Conference proceedings) and available at the NIH website (http://imagej.nih.gov/ij/macros/toolsets/Angiogenesis%20Analyzer.txt).

Protein production

Culture media (CM) from CLEC14A-Fc expressing HEK293T cells was collected. CM was flowed over a HiTrap protein A HP column (GE healthcare, Amersham, UK) and protein eluted using a 0-100 % gradient of 100 mM sodium citrate (pH 3) before neutralising with 1 M Tris base. Fractions were run on a SDS-PAG and assessed for protein purity and specificity by Coomassie staining and Western blotting. Fractions containing similar concentrations of protein were combined and dialysed in PBS prior to functional assays.

Monoclonal antibody generation

Mouse monoclonal antibodies were commercially prepared by Serotec Ltd (Oxford, UK) using the following protocol to break tolerance supplied by us. Purified mouse CLEC14A-Fc fusion protein was given at 50 μg in Freunds complete adjuvant subcutaneously. Two weeks later mice were given another 50 μg subcutaneously but this time in Freunds adjuvant. Mice were culled and spleens harvested for fusion two weeks later.

Generation of *clec14a*$^{-/-}$ mice

Mice were housed at the Birmingham Biomedical Services Unit (Birmingham, UK). C57BL/6N VGB6 feeder-dependent embryonic stem cells containing the CLEC14A deletion cassette (Clec14atm1(KOMP)Vlcg; project ID VG10554) were procured from the Knockout Mouse Project (University of California, Davis, USA). The Transgenic Mouse Facility at the

University of Birmingham generated chimeric mice by injection of embryonic stem cells into albino C57BL/6 mice and were bred to C57BL/6 females to generate mice heterozygous for the cassette. Animal maintenance had appropriate Home Office approval and licensing.

Aortic ring and murine subcutaneous sponge angiogenesis assay

Aortas were isolated and processed for aortic ring assays in collagen as previously described.[30] Tube/sprout outgrowth, maximal endothelial migration and total endothelial outgrowth was quantitated. The murine subcutaneous sponge angiogenesis assay was performed as previously described,[31] with slight modification. Male C57 black mice were implanted with a subcutaneous sterile polyether sponge disc (10×5×5 mm) under the dorsal skin of each flank at day 0. 100 μl bFGF (40 ng/ml; R&D systems) was injected through the skin directly into the sponges every other day for 14 days. Sponges were excised on day 14, fixed in 10 % formalin, and paraffin embedded. Sections were stained with haematoxylin and eosin, sponge cross-sections were taken using a Leica MZ 16 microscope (Leica, Milton Keynes, UK) with a USB 2.0 2M Xli digital camera at ×1 magnification for cellular invasion analysis. Images captured by Leica DM E microscope (Leica, Milton Keynes, UK) at 40× magnification were analysed for vessel density. Vessel counts were assessed in five fields per section per sponge. All animal experimentation was carried out in accordance with Home Office License number PPL 40/3339 held by RB.

Tumour implantation assays

10^6 Lewis lung carcinoma cells were injected subcutaneously into the flank of male mice at 8-10 weeks of age. Tumour growth was monitored by daily calliper measurements and after two-four weeks growth, tumour mass was determined by weight, fixed in 4 % PFA, paraffin embedded and serial sections cut at 6 μm.

Immunofluorescence and X-gal staining

Immunofluorescence staining was performed as previously described.[9]

X-Gal staining was performed as previously described.[32]

Supplementary Material

Refer to Web version on PubMed Central for supplementary material.

Acknowledgements

We thank Dr Laurens van der Flier, Somantix, and Dr Raj Mehta, Cancer Research Technology for helpful discussions. PN was supported by project grant number C4719/A6766 from Cancer Research UK to RB. The Portuguese Fundacao para a Ciencia e tecnologia funded AV. XZ was supported by a knowledge transfer partnership (KTP007696) from the Technology Strategy Board. PL is funded by MRC and the University of Birmingham and KK is funded by the University of Birmingham.

Funding: PN was funded by Cancer Research UK (CRUK, grant number C4719/A6766 to RB). AV was funded by the Portuguese Fundacao para a Ciencia and tecnologia. XZ was funded by a knowledge transfer partnership (KTP007696) from the Technology Strategy Board. PL is funded by MRC and the University of Birmingham and KK is funded by the University of Birmingham. The University of Birmingham Transgenic Mouse Facility is part of the MRC Centre for Immune Regulation.

References

1. Ziyad S, Iruela-Arispe ML. Molecular mechanisms of tumor angiogenesis. Genes Cancer. 2011; 2:1085–1096. [PubMed: 22866200]
2. Welti J, Loges S, Dimmeler S, Carmeliet P. Recent molecular discoveries in angiogenesis and antiangiogenic therapies in cancer. J Clin Invest. 2013; 123:3190–3200. [PubMed: 23908119]
3. De Bock K, Georgiadou M, Schoors S, Kuchnio A, Wong BW, Cantelmo AR, et al. Role of PFKFB3-driven glycolysis in vessel sprouting. Cell. 2013; 154:651–663. [PubMed: 23911327]
4. Jin H, Garmy-Susini B, Avraamides CJ, Stoletov K, Klemke RL, Varner JA. A PKA-Csk-pp60Src signaling pathway regulates the switch between endothelial cell invasion and cell-cell adhesion during vascular sprouting. Blood. 2010; 116:5773–5783. [PubMed: 20826718]
5. Bignon M, Pichol-Thievend C, Hardouin J, Malbouyres M, Bréchot N, Nasciutti L, et al. Lysyl oxidase-like protein-2 regulates sprouting angiogenesis and type IV collagen assembly in the endothelial basement membrane. Blood. 2011; 118:3979–3989. [PubMed: 21835952]
6. Welch-Reardon KM, Ehsan SM, Wang K, Wu N, Newman AC, Romero-Lopez M, et al. Angiogenic sprouting is regulated by endothelial cell expression of Slug. J Cell Sci. 2014; 127:2017–2018. [PubMed: 24554431]
7. Bergers G, Hanahan D. Modes of resistance to anti-angiogenic therapy. Nat Rev Cancer. 2008; 8:592–603. [PubMed: 18650835]
8. Zelensky AN, Gready JE. The C-type lectin-like domain superfamily. FEBS J. 2005; 272:6179–6217. [PubMed: 16336259]
9. Mura M, Swain RK, Zhuang X, Vorschmitt H, Reynolds G, Durant S, et al. Identification and angiogenic role of the novel tumor endothelial marker CLEC14A. Oncogene. 2012; 31:293–305. [PubMed: 21706054]
10. Rho S-S, Choi H-J, Min J-K, Lee H-W, Park H, Park H, et al. Clec14a is specifically expressed in endothelial cells and mediates cell to cell adhesion. Biochem Biophys Res Commun. 2011; 404:103–108. [PubMed: 21095181]
11. Zanivan S, Maione F, Hein MY, Hernández-Fernaud JR, Ostasiewicz P, Giraudo E, et al. SILAC-based proteomics of human primary endothelial cell morphogenesis unveils tumor angiogenic markers. Mol Cell Proteomics. 2013; 12:3599–3611. [PubMed: 23979707]
12. Ki MK, Jeoung MH, Choi JR, Rho S-S, Kwon Y-G, Shim H, et al. Human antibodies targeting the C-type lectin-like domain of the tumor endothelial cell marker clec14a regulate angiogenic properties in vitro. Oncogene. 2013; 32:5449–5457. [PubMed: 23644659]
13. Masiero M, Simões FC, Han HD, Snell C, Peterkin T, Bridges E, et al. A Core Human Primary Tumor Angiogenesis Signature Identifies the Endothelial Orphan Receptor ELTD1 as a Key Regulator of Angiogenesis. Cancer Cell. 2013; 24:229–241. [PubMed: 23871637]
14. Sanz-Moncasi MP, Garin-Chesa P, Stockert E, Jaffe EA, Old LJ, Rettig WJ. Identification of a high molecular weight endothelial cell surface glycoprotein, endoGlyx-1, in normal and tumor blood vessels. Lab Invest. 1994; 71:366–373. [PubMed: 7933987]
15. Colombatti A, Spessotto P, Doliana R, Mongiat M, Bressan GM, Esposito G. The EMILIN/Multimerin Family. Front Immunol. 2011; 2:93. [PubMed: 22566882]
16. Cullen M, Seaman S, Chaudhary A, Yang MY, Hilton MB, Logsdon D, et al. Host-derived tumor endothelial marker 8 promotes the growth of melanoma. Cancer Res. 2009; 69:6021–6026. [PubMed: 19622764]
17. Düwel A, Eleno N, Jerkic M, Arevalo M, Bolaños JP, Bernabeu C, et al. Reduced tumor growth and angiogenesis in endoglin-haploinsufficient mice. Tumour Biol. 2007; 28:1–8. [PubMed: 17108712]
18. Thijssen VLJL, Postel R, Brandwijk RJMGE, Dings RPM, Nesmelova I, Satijn S, et al. Galectin-1 is essential in tumor angiogenesis and is a target for antiangiogenesis therapy. Proc Natl Acad Sci USA. 2006; 103:15975–15980. [PubMed: 17043243]
19. Nanda A, Karim B, Peng Z, Liu G, Qiu W, Gan C, et al. Tumor endothelial marker 1 (Tem1) functions in the growth and progression of abdominal tumors. Proc Natl Acad Sci USA. 2006; 103:3351–3356. [PubMed: 16492758]

20. Nanda A, St Croix B. Tumor endothelial markers: new targets for cancer therapy. Curr Opin Oncol. 2004; 16:44–49. [PubMed: 14685092]
21. Pircher A, Fiegl M, Untergasser G, Heidegger I, Medinger M, Kern J, et al. Favorable prognosis of operable non-small cell lung cancer (NSCLC) patients harboring an increased expression of tumor endothelial markers (TEMs). Lung Cancer. 2013; 81:252–258. [PubMed: 23664449]
22. Zhuang X, Cross D, Heath VL, Bicknell R. Shear stress, tip cells and regulators of endothelial migration. Biochem Soc Trans. 2011; 39:1571–1575. [PubMed: 22103489]
23. Stapor PC, Wang W, Murfee WL, Khismatullin DB. The distribution of fluid shear stresses in capillary sprouts. Cardiovasc Eng Tech. 2011; 2:124–136.
24. Chaudhary A, Hilton MB, Seaman S, Haines DC, Stevenson S, Lemotte PK, et al. TEM8/ANTXR1 blockade inhibits pathological angiogenesis and potentiates tumoricidal responses against multiple cancer types. Cancer Cell. 2012; 21:212–226. [PubMed: 22340594]
25. Aricescu AR, Lu W, Jones EY. A time- and cost-efficient system for high-level protein production in mammalian cells. Acta Crystallogr D Biol Crystallogr. 2006; 62:1243–1250. [PubMed: 17001101]
26. Maciag T, Cerundolo J, Ilsley S, Kelley PR, Forand R. An endothelial cell growth factor from bovine hypothalamus: identification and partial characterization. Proc Natl Acad Sci USA. 1979; 76:5674–5678. [PubMed: 293671]
27. Pfaffl MW. A new mathematical model for relative quantification in real-time RT-PCR. Nucleic Acids Res. 2001; 29:2002–2007.
28. Desjobert C, Noy P, Swingler TE, Williams H, Gaston K, Jayaraman P-S. The PRH/Hex repressor protein causes nuclear retention of Groucho/TLE co-repressors. Biochem J. 2009; 417:121–132. [PubMed: 18713067]
29. Korff T, Krauss T, Augustin HG. Three-dimensional spheroidal culture of cytotrophoblast cells mimics the phenotype and differentiation of cytotrophoblasts from normal and preeclamptic pregnancies. Exp Cell Res. 2004; 297:415–423. [PubMed: 15212944]
30. Baker M, Robinson SD, Lechertier T, Barber PR, Tavora B, D'Amico G, et al. Use of the mouse aortic ring assay to study angiogenesis. Nat Protoc. 2011; 7:89–104. [PubMed: 22193302]
31. Suchting S, Heal P, Tahtis K, Stewart LM, Bicknell R. Soluble Robo4 receptor inhibits in vivo angiogenesis and endothelial cell migration. FASEB J. 2005; 19:121–123. [PubMed: 15486058]
32. Saunders TL. Reporter molecules in genetically engineered mice. Methods Mol Biol. 2003; 209:125–143. [PubMed: 12357949]
33. Lorenzon E, Colladel R, Andreuzzi E, Marastoni S, Todaro F, Schiappacassi M, et al. MULTIMERIN2 impairs tumor angiogenesis and growth by interfering with VEGF-A/VEGFR2 pathway. Oncogene. 2012; 31:3136–3147. [PubMed: 22020326]
34. Wilson E, Leszczynska K, Poulter NS, Edelmann F, Salisbury VA, Noy PJ, et al. RhoJ interacts with the GIT-PIX complex and regulates focal adhesion disassembly. J Cell Sci. 2014; 127:3039–3051. [PubMed: 24928894]

Europe PMC Funders Author Manuscripts

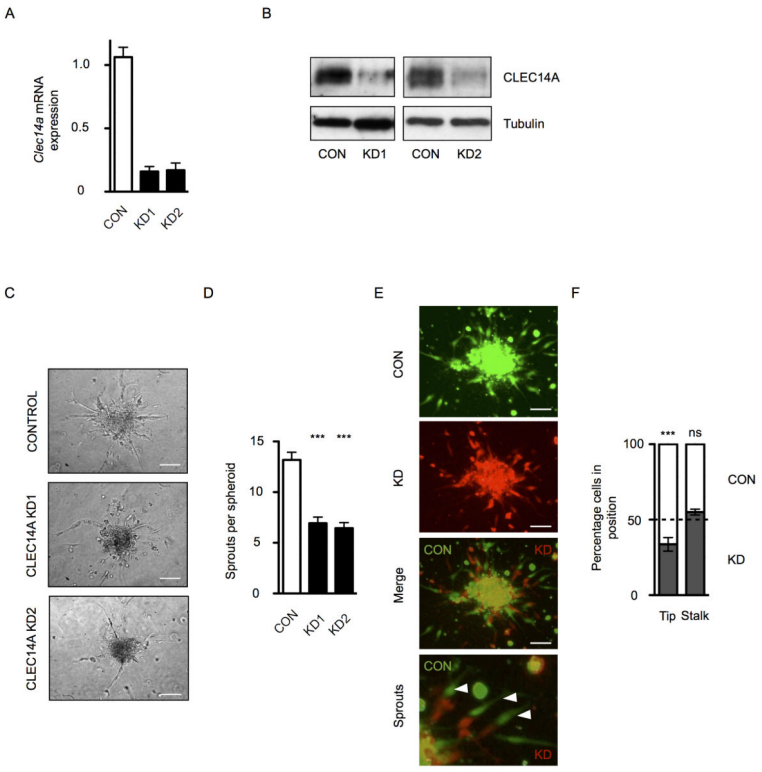

Figure 1.

SiRNA knockdown of CLEC14A reveals a role for CLEC14A in endothelial sprouting. [A] SiRNA duplexes targeting CLEC14A can efficiently knockdown CLEC14A mRNA expression in HUVEC, as determined by qPCR. Relative expression was determined by normalising expression to *flotillin2*. [B] Knockdown of CLEC14A at the protein level was determined for both siRNAs by Western blot analysis. Tubulin was used as a loading control. [C] Representative images of sprout outgrowth after 16 hours for control or *clec14a* targeted siRNA treated HUVEC. Scale bars are equal to 100 μm. [D] Quantitation of sprouts for 27 spheroids (9 spheroids from 3 cords) for control and CLEC14A knockdown HUVEC; Kruskal-Wallis statistical test $p<0.001$. [E] Representative images of sprout outgrowth after 24 hours for mixed control (green) and *clec14a* targeted siRNA treated HUVEC (red). Scale bars are equal to 100 μm. [F] Quantitation of the percentage of tip and stalk cells derived from control (CON) and CLEC14A knockdown (KD) HUVEC; two-way ANOVA statistical test with Bonferroni post-tests *** = $p<0.001$, ns = not significant.

Europe PMC Funders Author Manuscripts

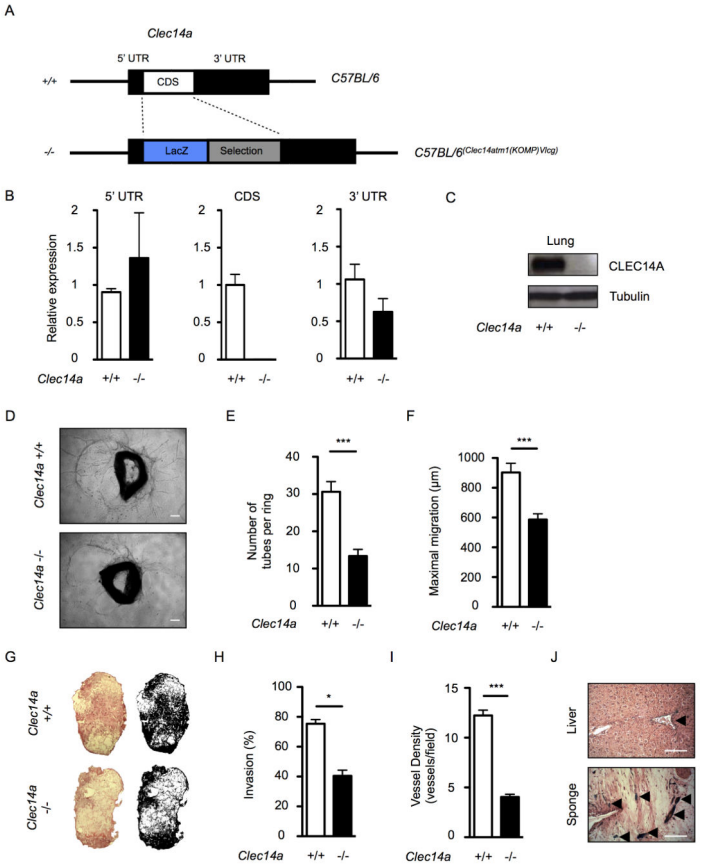

Figure 2.

Loss of CLEC14A inhibits sprouting *in vitro* and *in vivo*. [A] Schematic diagram of *clec14a* gene in C57BL/6 (*clec14a*$^{+/+}$) or C57BL/6$^{(Clec14atm1(KOMP)Vlcg)}$ (*clec14a*$^{-/-}$) mice. [B] Quantitative PCR analysis of cDNA generated from three *clec14a*$^{+/+}$ mice (white bars) and three *clec14a*$^{-/-}$ mice (black bars) for the 5′ untranslated region (UTR), coding sequence (CDS) and 3′ UTR of *clec14a*. Relative expression was determined by normalising expression to *flotillin2*. [C] Western blot analysis of CLEC14A protein expression in lung lysates from *clec14a*$^{+/+}$ and *clec14a*$^{-/-}$ mice using polyclonal antisera against murine CLEC14A. Tubulin was used as a loading control. [D] Representative images of the aortic ring sprouting assay from *clec14a*$^{+/+}$ and *clec14a*$^{-/-}$ mice. Scale bars are equal to 200 µm. Quantitation of tubes formed per ring [E], and quantitation of the longest distance migrated away from the aortic ring by an endothelial tube per aortic ring [F], data from 48 rings per genotype, 6 mice for each genotype; Mann-Whitney statistical test $p<0.001$. [G] Representative images of haematoxylin and eosin stained sections of sponge implant from *clec14a*$^{+/+}$ and *clec14a*$^{-/-}$ mice, sections at the centre of the sponge were analysed. Black and white images represent the masks generated during the threshold analysis for quantitation. [H] Quantitation of cellular invasion, by threshold analysis of haematoxylin and eosin stained cellular material within the sponge implants shown in G; Mann-Whitney statistical test $p<0.05$. [I] Quantitation of vessel density; Mann-Whitney statistical test $p<0.001$. [J] Sections of liver and sponge tissue stained with x-gal from *clec14a*$^{-/-}$ mice, counterstained with haematoxylin and eosin. Arrows indicate vessels stained with x-gal and

the increased intensity in the sponge tissue compared to the liver. Scale bars are equal to 100 μm.

Europe PMC Funders Author Manuscripts

Europe PMC Funders Author Manuscripts

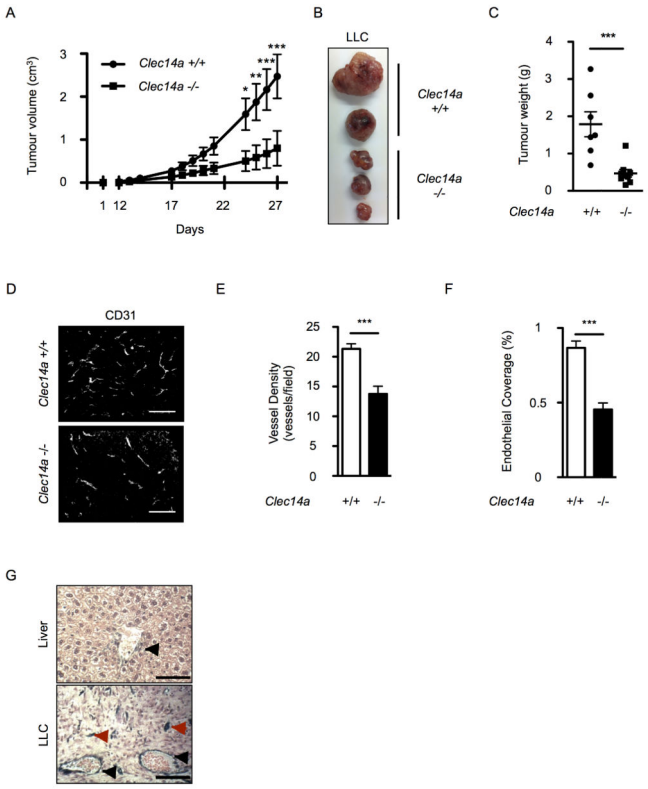

Figure 3.

Loss of CLEC14A inhibits tumour growth. [A] Lewis lung carcinoma (LLC) tumour growth in *clec14a*$^{+/+}$ (black line with dots) and *clec14a*$^{-/-}$ (black line with squares) mice; two-way ANOVA statistical analysis, * = p<0.05, ** = p<0.01, *** = p<0.001. [B] Representative images of LLC tumours. [C] Endpoint tumour weight for 7 *clec14a*$^{+/+}$ (dots) and 7 *clec14a*$^{-/-}$ (squares) mice; Mann-Whitney statistical test p<0.001. [D] Representative images of immunofluorescent staining of LLC tumour sections stained for murine CD31. Scale bars are equal to 100 μm. Quantitation of vessel density [E] and percentage endothelial coverage [F] from *clec14a*$^{+/+}$ and *clec14a*$^{-/-}$ mice; Mann-Whitney statistical test p<0.0001. [G] Sections of liver and LLC tumour tissue from *clec14a*$^{-/-}$ mice stained with x-gal, counterstained with haematoxylin and eosin. Scale bars are equal to 100 μm.

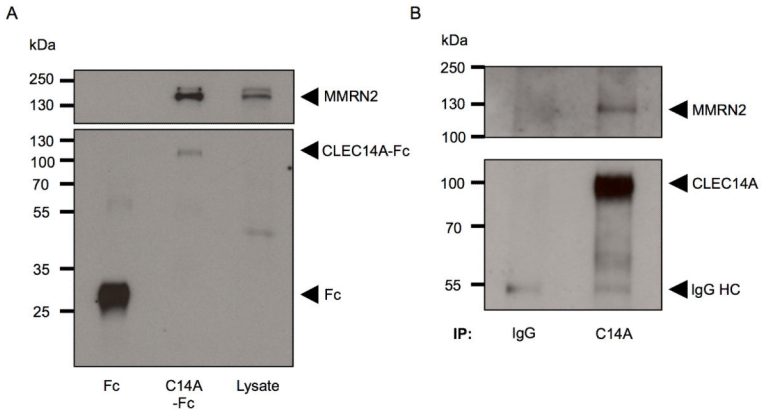

Figure 4.

MMRN2 binds to CLEC14A. [A] 20 μg CLEC14A-ECD-Fc or Fc was used to precipitate interacting partners. Precipitates and HUVEC lysates were separated on an SDS-PAG and blotted for MMRN2 (top panel) or CLEC14A-ECD-Fc (bottom panel). [B] CLEC14A was immunoprecipitated from HUVEC lysates using polyclonal antisera against CLEC14A. Immunoprecipitates were analysed by Western blot for MMRN2 (top panel) and CLEC14A (bottom panel).

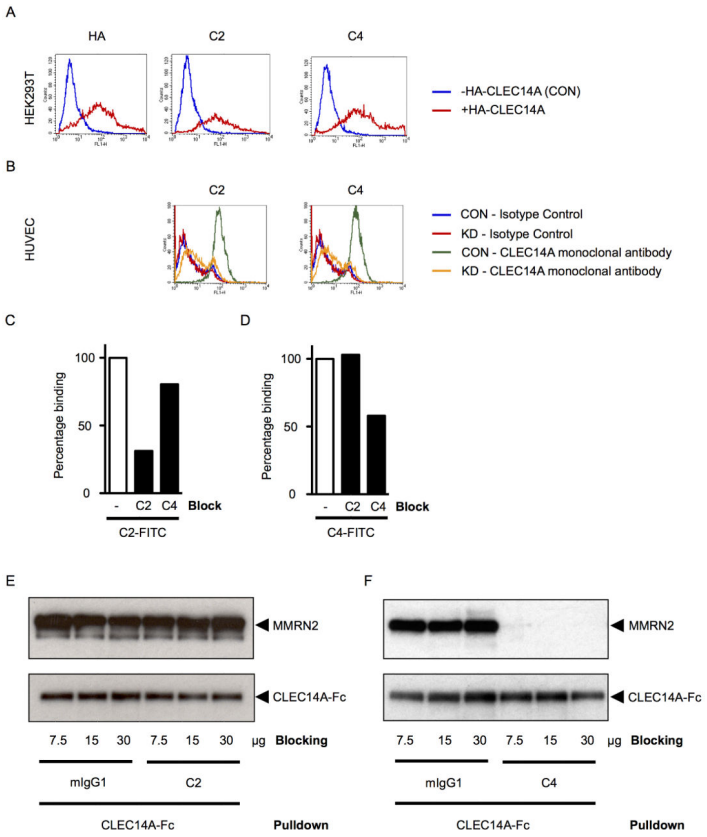

Figure 5.

CLEC14A monoclonal antibodies block MMRN2-CLEC14A interaction. [A] HEK293T cells expressing HA-CLEC14A or an empty vector (CON) were stained with an HA tag antibody (column 1), or monoclonal antibodies against CLEC14A C2 (column 2) or C4 (column 3). Cells were analysed by flow cytometry and displayed as histograms of increasing fluorescence (x-axis) versus counts (y-axis). [B] HUVECs transfected with negative control siRNA duplexes or siRNA duplexes targeting CLEC14A were probed with C2 or C4 antibodies and analysed as in A. [C] HUVECs were pre-treated with blocking buffer (−), 100 µg C2 antibody or 100 µg C4 antibody, prior to C2-FITC staining. Cells were analysed by flow cytometry. Geometric means were normalised to staining for the cells pre-treated with blocking buffer. [D] as for C, except stained with C4-FITC. [E] CLEC14A-Fc (5 µg) protein G agarose bead complexes were blocked with 7.5, 15, 30, µg mIgG or C2, prior to MMRN2 pulldown from HEK293T lysates. Precipitates were separated by SDS-PAGE and blotted for MMRN2 (upper panel) and CLEC14A-Fc (lower panel). [F] as in E, except C4 was used to block instead of C2.

Europe PMC Funders Author Manuscripts

Europe PMC Funders Author Manuscripts

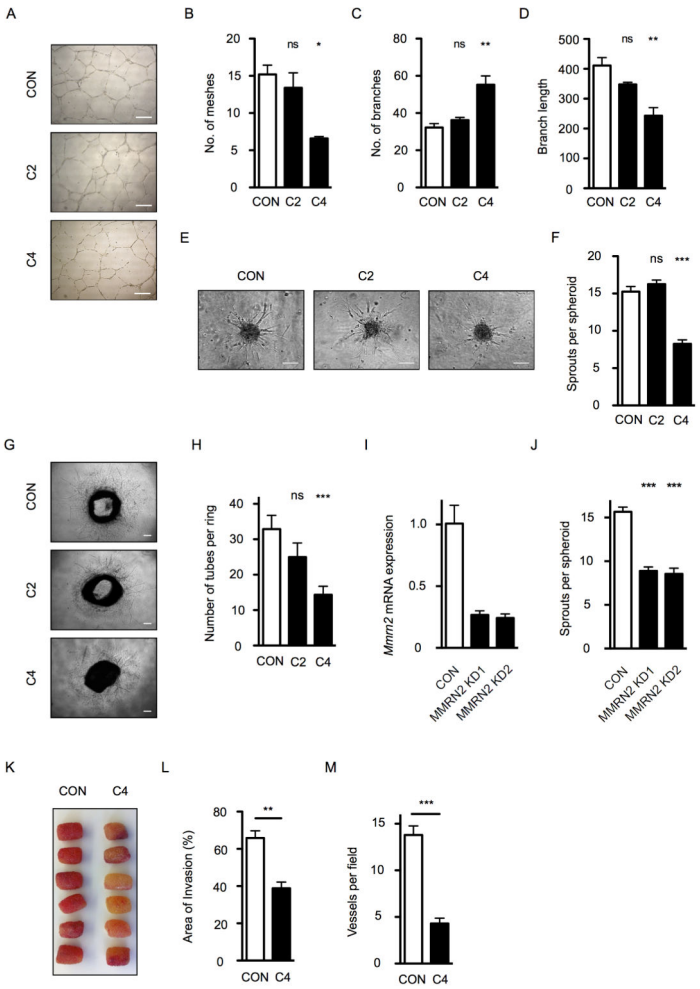

Figure 6.

MMRN2-CLEC14A interaction blocking antibody inhibits endothelial tube formation and sprouting *in vitro* and *in vivo*. HUVECs were plated onto Matrigel and grown in the presence of 20 μg/ml mIgG1 (CON), C2, or C4 antibodies for 16 hours. [A] Representative images. Scale bars are equal to 100 μm. Tube formation was analysed for number of meshes [B], number of branches [C] and the branch length [D]. Representative data from 1 of 3 independent experiments; Kruskal-Wallis statistical test, * = $p<0.05$, ** = $p<0.01$, ns = not significant. HUVEC spheroids embedded in a collagen gel were stimulated to sprout with VEGF supplemented with 20 μg/ml mIgG1 (CON), C2 or C4. [E] Representative images. Scale bars are equal to 100 μm. [F] Quantitation of sprouts per spheroid for 27 spheroids from 3 independent experiments; Kruskal-Wallis statistical test *** = $p<0.001$, ns = not significant. Aortic rings from C57BL/6 mice were cultured in the presence of 20 μg/ml mIgG1 (CON), C2 or C4. [G] Representative images. Scale bars are equal to 200 μm. [H] Quantitation of tubes formed per ring, data from 30 rings, at least 6 mice were used for each condition; Kruskal-Wallis statistical test *** = $p<0.001$, ns = not significant. [I] *Mmrn2* expression can be efficiently knocked down by siRNA duplexes in HUVEC, as determined by qPCR. Relative expression was determined by normalising expression to *flotillin2*. [J] Endothelial sprout outgrowth after 16 hours VEGF treatment of control or *mmrn2* targeted

siRNA treated HUVEC spheroids. Quantitation of sprouts for 27 spheroids (9 spheroids from 3 cords); Kruskal-Wallis statistical test $p<0.001$. [K] Representative images of sponge implants injected with bFGF and mIgG1 (CON) or C4 antibody. [L] Quantitation of cellular invasion into these sponge implants by threshold analysis of haematoxylin and eosin stained cellular material; Mann-Whitney statistical test $p<0.01$. [M] Quantitation of vessel density from K; Mann-Whitney statistical test $p<0.001$.

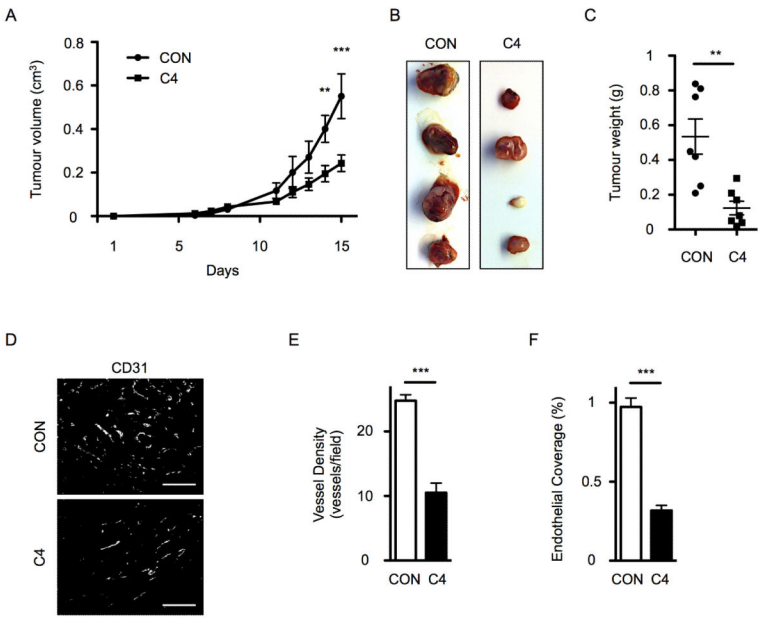

Figure 7.

MMRN2-CLEC14A interaction blocking antibody inhibits tumour growth. [A] Mice injected with LLC were treated with 100 μg injections of mIgG1 (black line with dots; n=7) or C4 antibody (black line with squares; n=7); two-way ANOVA statistical analysis, ** = $p<0.01$, *** = $p<0.001$. [B] Representative images of LLC tumours. [C] Endpoint tumour weight for 7 mIgG1 treated mice (dots) and 7 C4 antibody treated mice (squares); Mann-Whitney statistical test $p<0.001$. [D] Representative images of immunofluorescent staining of LLC tumour sections stained for murine CD31. Scale bars are equal to 100 μm. Quantitation of vessel density [E] and percentage endothelial coverage [F] from mice treated with mIgG1 or C4 antibody; Mann-Whitney statistical test $p<0.001$.

Europe PMC Funders Author Manuscripts

Europe PMC Funders Author Manuscripts

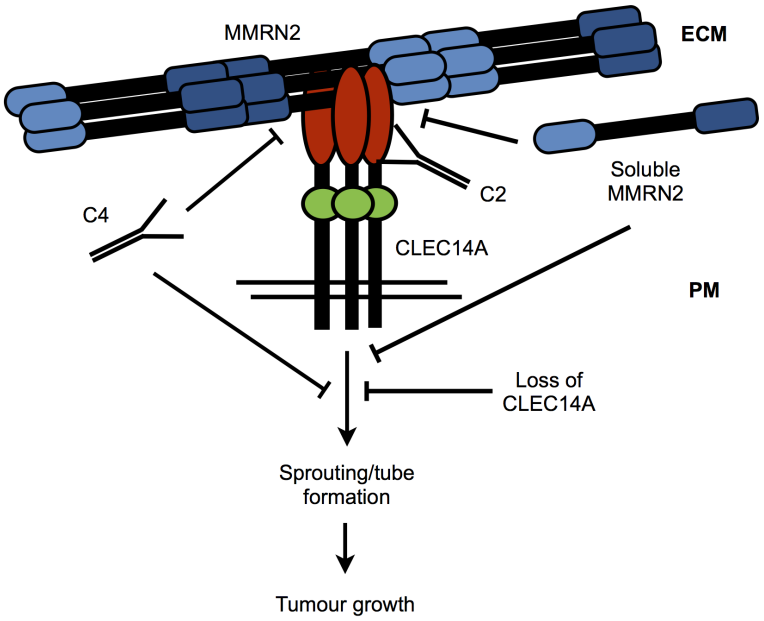

Figure 8.

CLEC14A-MMRN2 binding is an important component of endothelial sprout formation and a regulator of tumour growth. ECM = extracellular matrix, PM = plasma membrane.